The crystal structure of ingersonite, $Ca_3Mn^{2+}Sb_4^{5+}O_{14}$, and its relationships with pyrochlore

PAOLA BONAZZI* AND LUCA BINDI

Dipartimento di Scienze della Terra, Università degli Studi di Firenze, via La Pira 4, I-50121 Firenze, Italy

ABSTRACT

The crystal structure of ingersonite, $[Ca_{2.93}Mn^{2+}_{1.06}Fe^{2+}_{0.01}][Sb^{5+}_{3.95}Mg_{0.05}]F_{0.15}O_{13.85}$, has been solved and refined in the space group $P3_121$ [$a = 7.282(2)$, $c = 17.604(4)$ Å, $V = 808.4(3)$ Å^3, $Z = 3$] to $R = 2.32\%$ for 2219 $F_o > 4\sigma(F_o)$ using MoKα X-ray data.

The structure of ingersonite is isostructural with the synthetic weberite-3T polytype and related to the pyrochlore structure type. Both ingersonite and pyrochlore structures can be described as a sequence of pairs of polyhedral layers (named M and N), stacked along [111] and [001], respectively. In terms of the cation sites, M and N layers have general formula AB$_3$ and A$_3$B, respectively, where B are the octahedral cations forming the B$_2$X$_6$ framework of the pyrochlore structure and A are the larger, interstitial cations forming eightfold polyhedra in pyrochlore.

In ingersonite, the M layers occur at $z \sim 1/6$, 1/2, and 5/6: The B octahedra are occupied by Sb^{5+} and share corners to form a pseudohexagonal tungsten bronze (HTB) motif with the A position occupied by octahedral Mn^{2+} at the center of the pseudohexagonal rings. N layers occur at $z \sim 0$, 1/3, and 2/3, with A = Ca and B = Sb^{5+}: Isolated B octahedra share 6 edges with 6 eightfold A polyhedra, to form a continuous sheet similar to the analogous layer in pyrochlore. The stacking of successive pairs of M and N layers in ingersonite is the same as in pyrochlore. Nonetheless, a difference in the relative position between M and N layers in ingersonite and pyrochlore is observed. The crystal-chemical relationships with other pyrochlore-related minerals are outlined.

Keywords: Ingersonite, crystal structure, chemical data, weberite-3T polytype, pyrochlore-related structure, X-ray diffraction data

INTRODUCTION

Ingersonite, ideally $Ca_3Mn^{2+}Sb_4^{5+}O_{14}$, was found on the dumps at the Långban mine, Värmland, Sweden, associated with fine-grained calcite and two opaque minerals, jacobsite and filipstadite (Dunn et al. 1988). According to these authors, ingersonite is trigonal, with $a = 7.287(3)$ Å, $c = 17.679(9)$ Å, and $Z = 3$, with the single-crystal diffraction pattern exhibiting a primitive lattice, Laue symmetry $\bar{3}m$, and possible space groups including $P31m$, $P3m1$, $P312$, $P321$, $P\bar{3}1m$, $P\bar{3}m1$, $P3_121$, and $P3_221$.

The unit cell of ingersonite can easily be transformed by the matrix [–2/3 –4/3 1/3 | 4/3 2/3 1/3 | –2/3 2/3 1/3] into a pseudo-cubic cell closely resembling that of the pyrochlore-type structure. Indeed, a wide variety of minerals having an ideal stoichiometry A$_2$B$_2$X$_6$Y (A = Ca, Na, K, Sr, Ba, Sn^{2+}, Pb^{2+}, REE^{3+}, Y, Sb^{3+}, Bi^{3+}, U^{4+}, □; B = Nb, Ta, Ti^{4+}, less commonly Sb^{5+}, Fe^{3+}, Sn^{4+} and W^{6+}; X = O$^{2–}$, Y = O$^{2–}$, F$^–$, OH$^–$, □) possess a cubic pyrochlore-type structure (space group $Fd\bar{3}m$). A relative ordering of the A cations and vacancies, or the accommodation of different cations with different coordination requirements can induce a reduction in symmetry below that of the conventional ideal pyrochlore structure. These relations, in combination with the A$_2$B$_2$O$_7$ pyrochlore-like general formula, suggested that the ingersonite structure is a derivative of the pyrochlore structure type. Nonetheless, the synthetic $Ca_2Sb_2O_7$ compound crystallizes with both pyrochlore and orthorhombic weberite structure types (Brisse et al. 1972; Knop et al. 1980). It was hypothesized that the factors controlling a given antimonate to crystallize in one of these two competing structures (i.e., ionic radius and electro-negativity of the A cation) define weberite and pyrochlore fields, with $Ca_2Sb_2O_7$ in the transition zone and $Mn_2Sb_2O_7$ well within the pyrochlore-type field (Knop et al. 1980). According to Scott (1990), the synthetic $Mn_2Sb_2O_7$ compound, however, crystallizes with a trigonal, pyrochlore-related structure (space group $P3_121$) with unit-cell parameters $a = 7.1913(4)$, $c = 17.402(2)$ Å. On the other hand, two slightly different trigonal structures with space group $P3_121$ (i.e. zirconolite-3T and weberite-3T) are found for (A,B)$_4$X$_7$ compounds having a similar unit cell ($a \sim 7$ Å, $c \sim 17$–18 Å). According to the IMA-approved nomenclature scheme (Bayliss et al. 1989), zirconolite-3T is the three-layered trigonal polytypoid of $CaZrTi_2O_7$ (Mazzi and Munno 1983), the others being zirconolite-3O (Mazzi and Munno 1983) and -2M (Gatehouse et al. 1981). Two additional polytypes, zirconolite-4M and -6T have been recently synthesized (Smith and Lumpkin 1993; Coelho et al. 1997). The mineral weberite, Na_2MgAlF_7, has orthorhombic symmetry (Giuseppetti and Tadini 1978) and represents, to our knowledge, the only natural member belonging to the weberite-type polytypic series; nonetheless, a few different polytypes are known among synthetic weberite-type fluorides and oxides, including 2M, 4M, 3T (Yakubovich et al. 1994), and

* E-mail: pbcry@geo.unifi.it

947

$6T$ (Grey and Roth 2000). In this view, natural weberite itself is a $2O$ polytype.

To determine the crystal structure of ingersonite and its relations with the pyrochlore-type structure, a crystal from the type material (sample 163012, Smithsonian Institution, Washington, U.S.A.), made available to us by Pete Dunn, was examined using single-crystal X-ray diffraction methods.

EXPERIMENTAL METHODS

A single crystal of ingersonite was selected for the structural study and examined by X-ray diffraction. A preliminary search routine found 25 reflections readily indexed with a unit cell close to that reported by Dunn et al. (1988). Unit-cell dimensions, determined by least-squares refinement of the setting angles of 24 reflections were: $a = 7.282(2)$, $c = 17.604(4)$ Å, $V = 808.4(3)$ Å^3. To assure merging in all the Laue classes, a full diffraction sphere was collected. Intensities were treated for Lorentz and polarization effects and subsequently corrected for absorption following the semi-empirical method of North et al. (1968). Experimental details of the data collection are given in Table 1.

Structure solution and refinement

The equivalent structure factors were tentatively merged according to $\bar{3}$ (R_{int} = 4.20%), $\bar{3}m1$ (R_{int} = 4.30%) and $\bar{3}1m$ (R_{int} = 57.5%) point groups. The only systematic absence was $00l$, $l = 3n$ and no systematic absence was observed for hkl reflections. However, reflections with $-h + k + l = 3n$ appeared strong, suggesting a pseudo-R lattice, corresponding to the cubic F-lattice of the pyrochlore structure. Because we observed a high number of relatively intense reflections [5088 with $I > 12\sigma(I)$ of 15 660 collected reflections] violating the above rules, but none violating the systematic absence on $00l$ ($00l$: $l = 3n$), there was no ambiguity in the assignment of 3_1 (or 3_2) along [001]. Therefore, although statistical tests on the distribution of |E| values suggested the structure to be centrosymmetric, we considered the non-centrosymmetric $P3_1$, $P3_2$, $P3_121$, or $P3_121$ as possible space group choices.

As a first trial, we solved the structure assuming the lower symmetry $P3_1$ or $P3_2$. The positions of Sb, Mn, and Ca atoms were found using the Patterson interpretation of the SHELXS-97 package (Sheldrick 1997a); successive F_o-Fourier syntheses allowed us to locate O atoms yielding the expected unit-cell content of $Mn_3Ca_9Sb_{12}O_{42}$. The best agreement between observed and calculated structure factors was obtained for the right-handed $P3_1$ model rather than its enantiomorph $P3_2$. Structure refinement was performed using SHELXL-97 (Sheldrick 1997b). The structural model, however, showed high values in the correlation matrix between pairs of atoms which are equivalent in the space group $P3_121$. The structure refinement was then carried out in the higher symmetry. Site-scattering values were refined using scattering curves for ionized species (Ibers and Hamilton 1974) as

follows: Ca^{2+} vs. Mn^{2+} for the A sites, Sb^{5+} vs. Mg^{2+} for the B sites and O vs. $\square$ for the anion sites. All oxygen sites were found to be fully occupied, and the occupancy factors were then fixed to 1.00. The mean electron numbers at the cation sites were: 20.0(1), 25.0(1), 20.0(1), 51.0(1), 50.3(1), and 50.9(1) for A1, A2, A3, B1, B2, and B3 respectively. Refinement in space group $P3_121$ with anisotropic displacement parameters quickly converged to $R = 2.32\%$ for 2219 observed reflections [according to the criterion $F_o > 4\sigma(F_o)$] and $R = 2.83\%$ for all 2374 independent reflections. Fractional atomic coordinates and anisotropic displacement parameters are shown in Tables 2. Table 3[1] lists the observed and calculated structure factors.

Chemical composition

The same crystal used for the structural study was embedded in resin and polished for the chemical analysis that was performed by means of a Jeol JXA-8600 electron microprobe. Major and minor elements were determined at 15 kV accelerating voltage and 10 nA beam current, with 15 s as counting times. For the WDS analyses the following lines were used: F$K\alpha$, Mg$K\alpha$, Ca$K\alpha$, Mn$K\alpha$, Fe$K\alpha$, and Sb$L\alpha$. The estimated analytical precision is: ±0.70 for Sb, ±0.55 for Ca, ±0.40 for Mn, ±0.10 for F, and ±0.05 for Fe and Mg. The standards employed were: Sb-pure element (Sb), bustamite (Mn), diopside (Ca), ilmenite (Fe), olivine (Mg), and fluorite (F). The fragment was found to be rather homogeneous within analytical error, except for F which ranges from 0.0 to 0.94 wt%. As shown in Table 4, the average chemical data (six analyses on different spots) are within the ranges reported in the original description of ingersonite (Dunn et al. 1988).

One of the pitfalls in the study of the pyrochlore-like oxides is the derivation of a chemical formula from EMPA chemical analyses. In principle, there are three major problems: (1) the possibility of mixed valence for metals, (2) the possible presence of significant vacancies, and (3) the possible presence of OH$^-$ and/or H_2O in the structure. As for ingersonite in particular, if specific oxygen-fugacity conditions were to imply Sb to be in part trivalent, as found in stibiconite (Vitaliano and Mason 1952), this element might occupy the A sites; on the other hand, high values of oxygen fugacity could imply the presence of Fe^{3+} or even Mn^{3+} in the B sites. As pointed out by Dunn et al. (1988), it is therefore not possible to normalize the formula, with complete confidence, neither to any specific site nor to the charge sum. Based on the results of the refinement of the occupancy factors, we assumed no cation or anion vacancies occur and tentatively normalized the analytical data on the basis of $\Sigma(A + B) = 8$. The resulting formula was: $Ca_{2.93}Mn_{1.06}Fe_{0.01}Mg_{0.05}Sb_{3.95}F_{0.15}O_{13.85}$. With the assumption that Sb and (Mn + Fe) are present at the pentavalent and divalent oxidation states, respectively, the deficiency of positive charge due to a small excess of divalent cations is perfectly balanced by the substitution of F$^-$ for O^{2-} and does not require the presence of hydroxyl groups at the anion sites. Thus, also taking into account the results of occupancy refinement (see Table 2), the following crystal-chemical formula can be assumed with reasonable confidence: $[Ca_{2.93}Mn_{1.06}^{2+}Fe_{0.01}^{2+}][Sb_{3.95}^{5+}Mg_{0.05}]F_{0.15}O_{13.85}$.

DESCRIPTION OF THE STRUCTURE AND DISCUSSION

Coordination polyhedra

There are three independent octahedral sites (labeled B1, B2, and B3, by analogy with the pyrochlore structure) that accommodate Sb^{5+} with very minor substitution by lighter divalent cations at B2. Octahedra exhibit a binary (B1 and B2) or pseudo-binary (B3) symmetry, with mean distances (<B1-O> = 1.974, <B2-O> = 1.983, <B3-O> = 1.960 Å) close to the sum of the ionic radii for a Sb^{5+}-O bond (0.60 + 1.38 = 1.98 Å; Shannon 1976), which is consistent with the value observed in the structure of romeite [1.9647 Å, Matsubara et al. (1996)] and in the trigonal structure

---

TABLE 1. Experimental details of data collection and structure refinement

instrument	Enraf Nonius CAD4
radiation	Mo$K\alpha$
space group	$P3_121$
cell parameters	$a = 7.282(2)$ Å
	$c = 17.604(4)$ Å
	$V = 808.4(3)$ Å^3
crystal size (μm)	0.400 x 0.410 x 0.450
wavelength	Mo$K\alpha$(26 mA x 50 kV)
theta-range (°)	1–35
range of hkl	$-11 \leq h \leq 11$
	$-11 \leq k \leq 11$
	$-28 \leq l \leq 28$
scan mode	ω
scan width (°)	2.50
scan speed (°/min)	3.3
number of parameters	105
collected reflections	15660
independent refl.	2374
refl. with $F_o > 4\sigma(F_o)$	2219
R_{int} (%)	4.30
R_{obs} (%)	2.32
R_{all} (%)	2.83
$\Delta\rho_{max}$ (e/Å^3)	1.65
$\Delta\rho_{min}$ (e/Å^3)	−1.58
extinction correction	none

TABLE 2. Positional and displacement parameters for atoms in the structure of ingersonite

		x/a	y/b	z/c	U_{11}	U_{22}	U_{33}	U_{23}	U_{13}	U_{12}	U_{eq}	Site population
A1	3a	0	0.8444(4)	2/3	0.0064(4)	0.0091(4)	0.0076(3)	−0.0006(2)	−0.0013(3)	0.0032(2)	0.0080(2)	Ca^{2+}
A2	3b	0.8355(4)	0	5/6	0.0236(5)	0.0260(4)	0.0029(3)	0.0048(3)	0.0024(2)	0.0130(3)	0.0173(3)	Mn^{2+}
A3	6c	0.4989(3)	0.3518(2)	0.66075(4)	0.0105(3)	0.0079(4)	0.0093(2)	0.0022(2)	−0.0009(3)	0.0051(3)	0.0090(2)	Ca^{2+}
B1	3a	0.31881(6)	0	1/3	0.0044(1)	0.0037(1)	0.0012(1)	−0.00015(9)	−0.00007(4)	0.00186(6)	0.00320(6)	Sb^{5+}
B2	3b	0.32968(7)	0	5/6	0.0042(1)	0.0037(1)	0.0023(1)	−0.0002(1)	−0.00012(5)	0.00185(6)	0.00347(8)	$0.983(2)Sb^{5+} + 0.017 Mg^{2+}$
B3	6c	0.33428(6)	0.5019(1)	0.83499(1)	0.00389(9)	0.00344(8)	0.00215(8)	−0.00003(5)	−0.00014(6)	0.00221(8)	0.00299(6)	Sb^{5+}
O1	6c	0.1989(4)	0.2199(4)	0.1471(1)	0.0060(9)	0.0120(9)	0.0112(9)	−0.0013(7)	−0.0002(7)	0.0052(8)	0.0096(4)	O^{2-}
O2	6c	0.5543(4)	0.6091(4)	0.2034(1)	0.0176(9)	0.0081(9)	0.0086(8)	−0.0017(8)	−0.0050(7)	0.0080(9)	0.0107(4)	O^{2-}
O3	6c	0.1975(4)	0.6399(4)	0.1489(1)	0.0050(9)	0.0079(9)	0.0106(8)	0.0003(8)	−0.0010(7)	0.0001(8)	0.0092(4)	O^{2-}
O4	6c	−0.0399(3)	0.3091(4)	0.0573(1)	0.0096(9)	0.0093(9)	0.0058(7)	−0.0007(7)	−0.0006(6)	0.0049(9)	0.0082(4)	O^{2-}
O5	6c	−0.0541(3)	0.8050(7)	0.0566(1)	0.0051(8)	0.0099(9)	0.0053(7)	−0.0010(9)	−0.0021(6)	0.0029(9)	0.0071(3)	O^{2-}
O6	6c	0.5437(7)	0.4046(4)	0.0560(1)	0.0085(9)	0.0081(8)	0.0032(7)	0.0015(6)	0.0015(9)	0.0026(9)	0.0073(4)	O^{2-}
O7	6c	0.5347(7)	0.7988(7)	0.0599(1)	0.0137(9)	0.0084(9)	0.0037(7)	0.0000(9)	0.0022(9)	0.0084(8)	0.0073(4)	O^{2-}

of the synthetic $Mn_2Sb_2O_7$ [1.99, 1.99, and 1.93 Å; Scott (1990)]. There are three independent sites hosting the divalent cations (labeled A1, A2, and A3 by analogy with the pyrochlore structure). A1 and A3 are occupied by Ca, which links eight oxygen atoms with bond distances ranging from 2.426 to 2.669Å (<A1-O> = 2.539 Å) and from 2.260 to 2.712 Å (<A3-O> = 2.504 Å), respectively. The resulting coordination polyhedron is a slightly distorted cube in the case of A1, whereas the polyhedron around A3 can be described as an irregular bicapped octahedron. The A2 site is completely occupied by Mn^{2+} that bonds to six oxygen atoms to form a tetragonally distorted (2 + 4) octahedron with the axial compression along [001]. Two other oxygen atoms (O2 × 2) lie approximately on the equatorial plane at 2.884 Å. The O2 atom loses its tetrahedral configuration, which characterizes all anions in the ideal pyrochlore structure.

The mean octahedral distance <A2-O> (2.305 Å) is greater than the value corresponding to the sum of the ionic radii for a Mn^{2+}-O bond [0.83 + 1.38 = 2.21 Å; Shannon (1976)], allowing therefore to exclude the presence of Mn^{3+} on this site, in spite of the marked axial compression which could involve crystal field stabilization for the $3d^4$ configuration of Mn^{3+}. Rather long <Mn^{2+}-O>^{VI} bond distances are also observed in the corresponding A polyhedra (i.e., Mn1, Mn2, Mn3) of the synthetic $Mn_2Sb_2O_7$ (2.41, 2.30, and 2.34 Å, respectively; Scott 1990). Bond distances and bond valences in the ingersonite structure are given in Tables 5 and 6, respectively.

Layered arrangement and comparison with pyrochlore-type structure

Both pyrochlore and ingersonite structures can be described as a sequence of pairs of polyhedral layers [hereafter named *M* and *N* following the same notation used by Mazzi and Munno (1983)], stacked along [111] and [001], respectively. As far as the cation sites are concerned, *M* and *N* layers have general formula AB₃ and A₃B, respectively, where B are the octahedrally coordinated cations forming the B_2X_6 framework of the pyrochlore structure and A are the larger, interstitial cations forming eightfold AY_2X_6 polyhedra in pyrochlore.

In the *M* layer the B octahedra share corners to form a pseudohexagonal tungsten bronze (HTB) motif forming empty triangular rings and A-centered, hexagonal (puckered) rings; due to the octahedral coordination of the A2 cation (A2 = Mn^{2+}), in the *M* layer of ingersonite the pseudohexagonal (trigonal) symmetry is lost (Fig. 1a), whereas in pyrochlore (Fig. 1b)

TABLE 4. Analytical data for ingersonite from the type locality

Oxide wt%	a	b
CaO	18.50	15.90–19.90
MnO	8.45	9.1–9.4
MgO	0.21	0.0–0.3
FeO	0.08	0.0–0.3
Sb_2O_5	72.03	72.6–74.7
F	0.32	1.4–1.3
Total	99.59	
−O=F	0.14	
Total	99.45	

Note: Column a = crystal used for the structural study (average of six analyses); column b = range of chemical variation reported in the original description of the mineral (Dunn et al. 1988).

the A cation (site symmetry $\bar{3}m$) forms a hexagonal puckered AY_2X_6 bipyramid. The link between B octahedra, however, is rather inflexible, resulting in high distortion of the MnO_6 polyhedron [$\lambda_{oct.}$ = 1.0111; σ^2_{oct} = 270.0, calculated according to the formulae given by Robinson et al. (1971)] but only minor modifications of the rings [O1-O1-O2 (×2) = 126.9, O1-O2-O3 (×2) = 105.9, O2-O3-O3 (×2) = 127.1°]. Only two edges (i.e., O1-O1 and O3-O3) are shared between the A2 polyhedra and B octahedra, thus forming $A2O_6$-$B2O_6$ strips held together by sharing corners with B3 octahedra. Successive *M* layers at $z \sim$ 1/6, $z \sim$ 1/2, and $z \sim$ 5/6 have strips directed along [010], [$\bar{1}$10], and [100], respectively.

The *N* layer of ingersonite (Fig. 2a) is very similar to the homologous layer of pyrochlore (Fig. 2b), although the latter shows a more regular arrangement: Isolated B1 octahedra share six edges with as many eightfold A polyhedra (two A1 and four A3), to form a continuous sheet made of parallel $A3O_8$-$B1O_6$ strips which alternate with $A1O_8$-$A3O_8$ strips. Successive *N* layers at $z \sim 0$, $z \sim 1/3$, and $z \sim 2/3$ have strips directed along [010], [$\bar{1}$ $\bar{1}$0], and [100] respectively.

White (1984) adopted a modular approach in describing pyrochlore and other pyrochlore-related structures (zirconolite polytypoids and related phases) having an octahedral framework arranged as HTB motifs. According to this author, the stacking sequence of successive HTB layers (i.e., *M* layers) can be described by two parameters *SV* and *SA*, where *SV* is the vector, projected down the (pseudo) sixfold axis, between crystallographically similar atoms in adjacent layers, and *SA* is the angle between successive *SV*s. In ingersonite successive *M* layers are displaced with respect to each other along [001] by $SV = a\sqrt{3}/3$ (= 4.204 Å) and SA = 120°. Analogous values can

TABLE 5. Bond distances (Å) in the structure of ingersonite

A1–O4 (×2)	2.426(2)	A2–O5 (×2)	1.968(2)	A3–O4	2.260(2)
O5 (×2)	2.438(5)	O1 (×2)	2.449(3)	O4	2.325(3)
O1 (×2)	2.622(2)	O3 (×2)	2.499(3)	O5	2.433(5)
O6 (×2)	2.669(5)	mean	2.305	O7	2.522(4)
mean	2.539			O3	2.549(2)
				O6	2.590(4)
				O7	2.641(5)
				O2	2.712(3)
				mean	2.504
B1–O5 (×2)	1.945(2)	B2–O4 (×2)	1.942(2)	B3–O3	1.951(3)
O7 (×2)	1.974(2)	O1 (×2)	2.003(3)	O1	1.955(3)
O6 (×2)	2.004(2)	O3 (×2)	2.005(3)	O7	1.959(2)
mean	1.974	mean	1.983	O2	1.961(3)
				O2	1.964(3)
				O6	1.970(2)
				mean	1.960

TABLE 6. Bond-valence (v.u.) arrangement for ingersonite

	A1	A2	A3	B1	B2	B3	
O1	$0.180^{×2}\downarrow$	$0.177^{×2}\downarrow$			$0.754^{×2}\downarrow$	0.872	1.983
O2			0.150			0.856	1.855
						0.849	
O3		$0.158^{×2}\downarrow$	0.210		$0.750^{×2}\downarrow$	0.883	2.001
O4	$0.274^{×2}\downarrow$		0.402		$0.908^{×2}\downarrow$		1.929
			0.345				
O5	$0.267^{×2}\downarrow$	$0.603^{×2}\downarrow$	0.270	$0.900^{×2}\downarrow$			2.040
O6	$0.164^{×2}\downarrow$		0.193	$0.752^{×2}\downarrow$		0.833	1.942
O7			0.222	$0.823^{×2}\downarrow$		0.862	2.080
			0.173				
	1.770	1.877	1.965	4.949	4.824	5.155	

Notes: bond strengths are calculated according to Brown and Wu (1976); x2 superscript indicates cations linking twice the same oxygen atom.
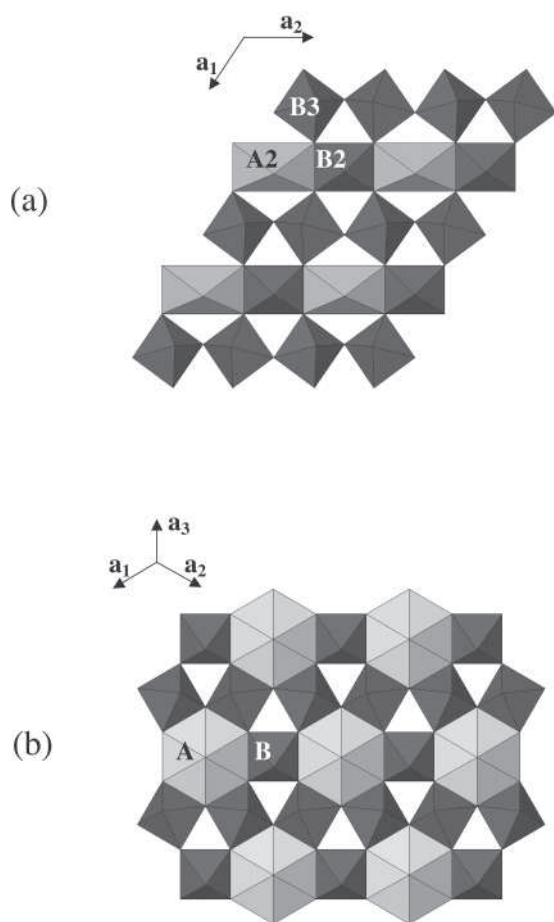

FIGURE 1. (**a**) *M* layer (at *z* ~ 1/6) in the structure of ingersonite (projection down [001]); (**b**) *M* layer in the structure of pyrochlore (projection down [111]).

be measured between successive *M* layers in pyrochlore along [111]. The displacement of successive *N* layers is described by the same *SV* and *SA* parameters in both the ingersonite and pyrochlore structures. Therefore, the stacking of successive pairs of *M* and *N* layers in ingersonite is the same as in pyrochlore. Nonetheless, there is a difference in the relative position between

M and *N* layers in ingersonite and pyrochlore. As an *M* layer is projected down the trigonal axis together with the underlying *N* layer, it appears that in ingersonite (Fig. 3a) the B1 octahedron is shifted ½[010] (at *z* ~ 0) with respect to the ideal position in pyrochlore, where the B octahedron belonging to the *N* layer lies just below the triangular ring of the *M* layer (Fig. 3b). In the successive *MN* pairs, the shift of the *N* layer with respect to the same layer in pyrochlore is ½[$\bar{1}$10] (at *z* ~ 1/3) and ½[100] (at *z* ~ 2/3). As a consequence of the difference in the relative position between *M* and *N* layers, the anions play a different crystal-chemical role in ingersonite with respect to pyrochlore. In the pyrochlore structure the X anions (48*f*) belong to the octahedral B_2O_6 framework, while the Y anion (8*b*) links only A cations, A-Y bonds being the axial bonds of the hexagonal puckered AY_2X_6 bipyramid of the pyrochlore structure. In ingersonite, on the contrary, the apical O atoms of the A2 polyhedra (i.e., O5), which in the *M* layer occupy the position corresponding to Y in pyrochlore, also link the B1 cation of an adjacent *N* layer. Therefore, in ingersonite there are no anion positions which are not linked to at least one octahedral B cation (Sb^{5+}). This feature makes an extensive (F^-, OH^-) → O^{2-} substitution in the structure of ingersonite rather difficult.

The difference in the relative position between *M* and *N* layers in ingersonite and pyrochlore can be also visualized by using an anion-centered polyhedral description. In these terms, the structure of pyrochlore can be described as anion-deficient fluorite derivative (Subramanian et al. 1984). The A and B cations form a face-centered cubic array with the anions occupying 7/8 of the tetrahedral interstices. On the contrary, in the ingersonite structure the anions occupy 6/8 of the tetrahedral and 1/4 of the octahedral interstices. In particular, one set of tetrahedral sites is fully occupied (4/4), while the other one is half occupied (2/4). The removed anion (i.e., the O2 atom) is relocated to the adjacent octahedral interstice. The arrangement of the X(A,B)₄ tetrahedra in ingersonite (Fig. 4a) differs from that observed in pyrochlore structure (Fig. 4b). Instead, the anion distribution among the interstitial cavities of the A_2B_2 array observed in ingersonite is identical to that observed in weberite-3*T* polytype (Fig. 4c). This arrangement, as well illustrated by Grey et al. (2003), is a common feature of all weberite-type polytypes. Therefore, the mineral
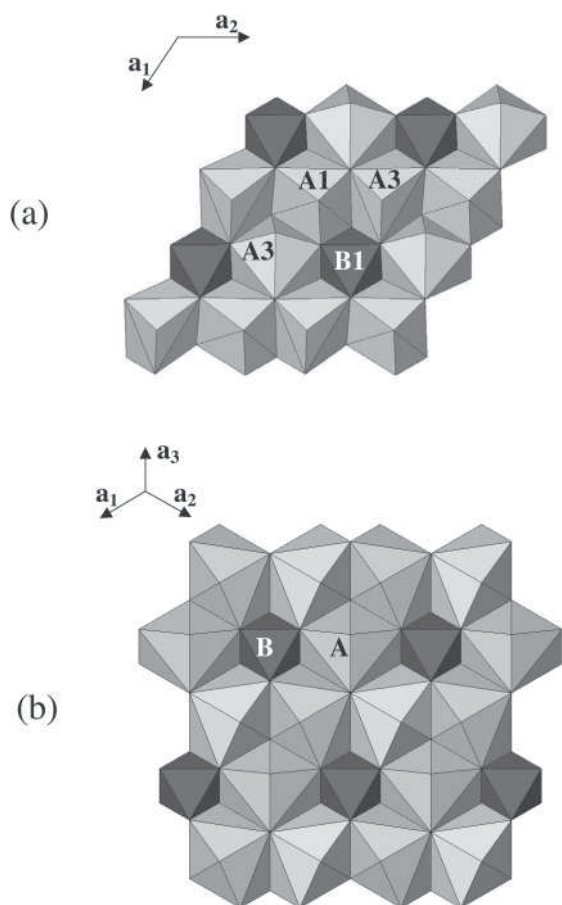
FIGURE 2. (**a**) N layer (at $z \sim 0$) in the structure of ingersonite (projection down [001]); (**b**) N layer in the structure of pyrochlore (projection down [111]).

FIGURE 3. BO_6 octahedra forming a HTB motif in the M layer of ingersonite (**a**) and pyrochlore (**b**) with the underlying N layer showing the difference in the relative position of the isolated BO_6 octahedron belonging to the N layer. Circles represent the A cations; in particular, smaller gray circles represent Mn^{2+} and larger white circles represent Ca.

ingersonite, as well as the synthetic $Mn_2Sb_2O_7$ (Scott 1990), are to be considered as more related to weberite than pyrochlore.

Zirconolite-$3T$ [^{VIII}(Ca, Na, REE,...)$_2$ ^{VII}Zr$_2$ ^{VI}(Ti, Nb,...)$_3$ ^{V,IV}(Fe,Ti)O$_{14}$, space group $P3_121$] exhibits a crystal structure similar, but not identical, to that of ingersonite. The M layer, in particular, is arranged as HTB motif, with B octahedra occupied by (Ti, Nb) cations and Fe asymmetrically located on a split position within the cavity which hosts Mn in ingersonite. The N layer differs due to a replacement of Zr on the A3 site of ingersonite, and (Ca, Na, REE) in both A1 and B1. Thus, the N layer in zirconolite-$3T$ appears to be made of strips of ZrO$_7$ edge-capped octahedra which alternate with CaO$_8$ strips. As in the case of ingersonite, in the zirconolite-$3T$ structure the anion corresponding to the Y site in pyrochlore is linked also to a highly charged cation (i.e., Zr^{4+}), thus preventing a significant amount of (F$^-$,OH$^-$) substitution for O^{2-}. In terms of anion-centered polyhedral description, however, zirconolite-$3T$ (Fig. 4d) appears to preserve the anion ordering on 7/8 of the tetrahedral interstices as observed in pyrochlore. Thus, in spite of the presence of irregular coordination polyhedra, zirconolite-$3T$ is more closely related to pyrochlore than weberites.
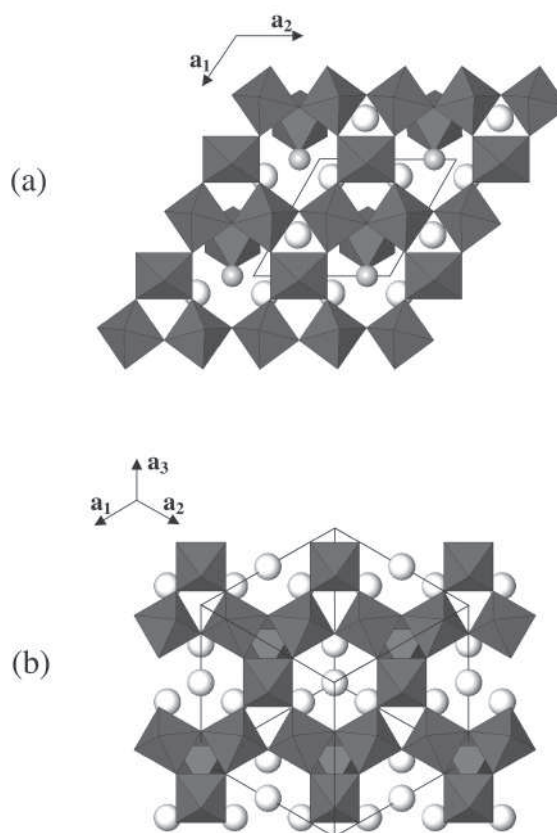
Another trigonal, pyrochlore-related mineral is parabariomicrolite, ideally Ba$\square_3$Ta$_4$O$_{10}$(OH)$_2\cdot$2H$_2$O: According to the structural model proposed by Ercit et al. (1986), parabariomicrolite crystallizes in the space group $R\bar{3}m$, with $a = 7.4290(6)$, $c = 18.502(2)$ Å. The ordering of Ba on one fourth of the A positions of the pyrochlore structure lowers the symmetry; nonetheless, the relative position of the M and N layers is maintained as in cubic pyrochlore, and the Y sites are still tetrahedrally surrounded by four A sites (one Ba and three $\square$), allowing the entry of H$_2$O and/or (F$^-$, OH$^-$) at this site. Accordingly, chemical data determined by electron microprobe reported in literature for parabariomicrolite show low analytical totals [92.3–94.5 wt% ox.; Ercit et al. (1986)].

Trigonal "pyrochlores": concluding remarks

The X-ray powder pattern calculated using the structural data obtained in this study is compared (Table 7) to that observed for the type material (Dunn et al. 1988). Taking into account the indexing based on the structural data, all reflections of the observed powder pattern display $-h + k + l = 3n$. Looking at the calculated pattern, only a few, weak reflections might reveal the P lattice of

TABLE 7. X-ray powder diffraction patterns for ingersonite

			1		2	
h	k	l	I_{calc}	d_{calc} (Å)	I/I_o	d_{obs} (Å)
1	0	0	2	6.306	–	–
1	0	1	6	5.937	–	–
0	0	3	16	5.868	20	5.89
0	1	2	12	5.126	10	5.12
1	0	2	3	5.126		
1	1	0	5	3.641	–	–
0	1	4	2	3.609	10	3.62
1	0	4	6	3.609		
1	1	1	2	3.566	–	–
1	1	2	3	3.365	–	–
0	2	1	13	3.104	20	3.10
1	1	3	2	3.094	–	–
0	1	5	2	3.074	–	–
2	0	2	100	2.969	100	2.965
0	0	6	32	2.934	–	–
0	2	4	40	2.563	40	2.565
2	1	4	3	2.096	1	2.093
0	0	9	2	1.956	2	1.965
2	2	0	29	1.821	50	1.820
2	0	8	26	1.805	50	1.810
2	2	3	3	1.739	2	1.742
3	1	2	2	1.716	1	1.714
0	4	2	12	1.552	60	1.549
2	2	6	22	1.547		
0	2	10	13	1.537	40	1.543
4	0	4	8	1.484	10	1.486
0	0	12	3	1.467	2	1.474
2	0	11	2	1.427	1	1.429
2	2	9	2	1.333	5	1.336
0	4	8	6	1.282	10	1.283
4	2	2	8	1.181	20	1.181
4	0	10	4	1.174	2	1.174
2	0	14	3	1.168	–	–
2	4	4	6	1.150	20	1.152
2	2	12	6	1.142	20	1.146
6	0	0	3	1.051	20	1.051
4	2	8	5	1.048	5	1.043
0	2	16	2	1.039	–	–

Notes: 1 = calculated powder pattern and indexing for ingersonite of this study. d values calculated on the basis of a = 7.282(2) Å, c = 17.604(4) Å, and with the structural data reported in Table 2. Intensities calculated using XPOW software version 2.0 (Downs et al. 1993). 2 = observed powder pattern originally reported by Dunn et al. (1988) re-indexed on the basis of structural data.

ingersonite: 100 (d = 6.31 Å; I_{calc} = 2.24), 111 (d = 3.57 Å; I_{calc} = 2.47), and 112 (d = 3.37 Å; I_{calc} = 2.75). Therefore, from powder diffraction alone, a trigonal, pyrochlore- or weberite-related compound likely appears to be rhombohedral irrespective of its proper P or R lattice. Many $A_2B_2O_7$ compounds were considered as "rhombohedrally distorted pyrochlores" on the basis of their diffraction powder pattern (Subramanian et al. 1983). Among them, the $(Mn_{1-x}Cd_x)_2Sb_2O_7$ phases (Subramanian et al. 1984) exhibit a rhombohedral unit cell for the Mn-rich members of the series (Mn > 0.8 apfu). As the pure $Mn_2Sb_2O_7$ phase (Scott 1990) crystallizes in the $P3_121$ space group with the weberite-$3T$ structure and no discontinuity is observed in the variation of unit-cell parameters along the join, it can be inferred that they maintain the weberite-$3T$ structure up the conversion to the cubic pyrochlore structure. It might indicate that the transition from weberite-$3T$ to pyrochlore type structure is related to the size of the A relative to B cations (ratio of mean ionic radii of $[A^{2+}]^{VIII}$ to $[B^{5+}]^{VI}$ in the range 1.60–1.74 for the trigonal phases). On the other hand, ingersonite itself (i.r.$[A^{2+}]^{VIII}$ / i.r. $[B^{5+}]^{VI}$ = 1.80) and the $Ca_{1.92}Nd_{0.08}Ta_{1.92}Zr_{0.08}O_7$ compound (i.r.$[A^{2+}]^{VIII}$/i.r. $[B^{5+}]^{VI}$ = 1.75) exhibit a weberite-$3T$ type structure (Grey et al. 2003), while the synthetic $Ca_2Sb_2O_7$ compound (i.r.$[A^{2+}]^{VIII}$/i.r. $[B^{5+}]^{VI}$ = 1.87) crystallizes with both pyrochlore and weberite-$2O$ structure types (Brisse et al. 1972; Knop et al. 1980). The $Y_2Mn_{2/3}^{2+}Mo_{4/3}^{5+}O_7$ and $Dy_2Mn_{4/3}^{3+}W_{2/3}^{6+}O_7$ compounds were identified as rhombohedral phases, whereas the $Y_2V_{4/3}^{3+}W_{2/3}^{6+}O_7$ compound appears to have a cubic pyrochlore structure, in spite of the similar sizes of V^{3+} and Mn^{3+} (Bazuev et al. 2006). According to the same authors, the $Y_2Cd_{2/3}^{2+}Re_{4/3}^{5+}O_7$ compound crystallizes in the space group $P3_121$, likely with zirconolite-$3T$ type structure. The reasons why some compounds do not adopt the cubic structure and which driving forces favor either weberite-$3T$ or zirconolite-$3T$ structure type are still unknown and require further study.
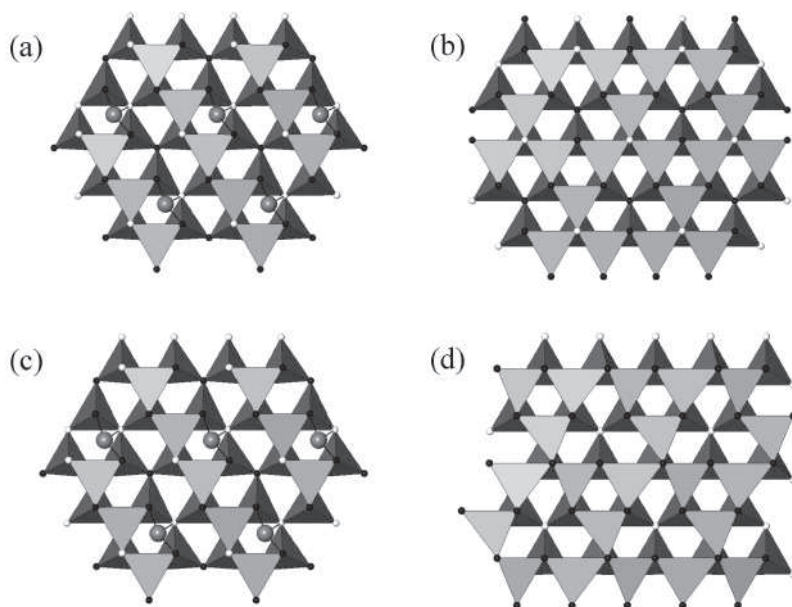

FIGURE 4. Arrangements of anion-centered X(A,B)$_4$ tetrahedra in ingersonite (**a**), pyrochlore-type structure (**b**), weberite-type polytypes (**c**), zirconolite-type polytypes (**d**). Black and white small circles represent A and B cations, respectively. Gray circles represent the three-coordinated oxygen atoms asymmetrically located in octahedral interstices.

REFERENCES CITED

Bayliss, P., Mazzi, F., Munno, R., and White, T.J. (1989) Mineral nomenclature: zirconolite. Mineralogical Magazine, 53, 565–569.

Bazuev, G.V., Chupakhina, T.I., Zubkov, V.G., Tyutyunnik, A.P., Zainulin, Yu.G., Neifeld, E.A., and Kadyrova, N.I. (2006) High-pressure synthesis and magnetic properties of complex oxide $Y_2Cd_{2/3}^{2+}Re_{4/3}^{5+}O_7$. Materials Research Bulletin, 41, 804–808.

Brisse, F., Stewart, D.J., Seidl, V., and Knop, O. (1972) Pyrochlores. VIII. Pyrochlores and related compounds and minerals. Canadian Journal of Chemistry, 50, 3648–3666.

Brown, I.D. and Wu, K.K. (1976) Empirical parameters for calculating cation-oxygen bond valences. Acta Crystallographica, B32, 1957–1959.

Coelho, A.A., Cheary, R.W., and Smith, K.L. (1997) Analysis and structural determination of Nd-substituted zirconolite-4M. Journal of Solid State Chemistry, 129, 346-359.

Downs, R.T., Bartelmehs, K.L., Gibbs, G.V., and Boisen, M.B., Jr. (1993) Interactive software for calculating and displaying X-ray or neutron powder diffractometer patterns of crystalline materials. American Mineralogist, 78, 1104–1107.

Dunn, P.J., Peacor, D.R., Criddle, A.J., and Stanley, C.J. (1988) Ingersonite, a new calcium-manganese antimonate related to pyrochlore, from Långban, Sweden. American Mineralogist, 73, 405–412.

Ercit, T.S., Hawthorne, F.C., and Černy, P. (1986) Parabariomicrolite, a new species and its structural relationship to the pyrochlore group. Canadian Mineralogist, 24, 655–663.

Gatehouse, B.M., Grey, I.E., Hill R.J., and Rossell H.J. (1981) Zirconolite, $CaZr_xTi_{3-x}O_7$; structure refinements for near-end-member compositions with $x = 0.85$ and 1.30. Acta Crystallographica, B37, 306–312.

Giuseppetti, G. and Tadini, C. (1978) Re-examination of the crystal structure of weberite. Tschermaks Mineralogische und Petrographische Mitteilungen, 25, 57–62.

Grey, I.E. and Roth, R.S. (2000) New calcium tantalate polytypes in the system $Ca_2Ta_2O_7$-$Sm_2Ti_2O_7$. Journal of Solid State Chemistry, 150, 167–177.

Grey, I.E., Mumme, W.G., Ness, T.J., Roth, R.S., and Smith, K.L. (2003) Structural relations between weberite and zirconolite polytypes—refinements of doped 3T and 4M $Ca_2Ta_2O_7$ and 3T $CaZrTi_2O_7$. Journal of Solid State Chemistry, 174, 285–295.

Knop, O., Demazeau, G., and Hagenmuller, P. (1980) Pyrochlores. XI. High-pressure studies of the antimonates $A_2Sb_2O_7$ ($A = Ca$, Sr, Cd) and preparation of the weberite $Sr_2Bi_2O_7$. Canadian Journal of Chemistry, 58, 2221–2224.

Ibers, J.A. and Hamilton, W.C., Eds. (1974) International Tables for X-ray Crystallography, vol. IV, 366 p. Kynock, Dordrecht, The Netherlands.

Matsubara, S., Kato, A., Shimizu, M., Sekiuchi, K., and Suzuki, Y. (1996) Romeite from the Gozaisho mine, Iwaki, Japan. Mineralogical Journal, 18, 155–160.

Mazzi, F. and Munno, R. (1983) Calciobetafite (new mineral of the pyrochlore group) and related minerals from Campi Flegrei, Italy; crystal structures of polymignyte and zirkelite: comparison with pyrochlore and zirconolite. American Mineralogist, 68, 262–276.

North, A.C.T., Phillips, D.C., and Mathews, F.S. (1968) A semiempirical method of absorption correction. Acta Crystallographica, A24, 351–359.

Robinson, K., Gibbs, G.V., and Ribbe, P.H. (1971) Quadratic elongation; a quantitative measure of distortion in coordination polyhedra. Science, 172, 567–570.

Scott, H.G. (1990) Refinement of the crystal structure of the manganese antimonate $Mn_2Sb_2O_7$ with neutron powder diffraction data by the profile decomposition method. Zeitschrift für Kristallographie, 190, 41–46.

Shannon, R.D. (1976) Revised effective ionic radii and systematic studies of interatomic distances in halides and chalcogenides. Acta Crystallographica, A32, 751–767.

Sheldrick, G.M. (1997a) SHELXS-97. A program for automatic solution of crystal structures. University of Göttingen, Germany.

——— (1997b) SHELXL-97. A program for crystal structure refinement. University of Göttingen, Germany.

Smith, K.L. and Lumpkin, G.R. (1993) Structural features of zirconolite, hollandite and perovskite, the major waste-bearing phases in Synroc. In Bolan, J.N. and FitzGerald, J.D., Eds., Defects and Processes in the Solid State: Geoscience Applications, p. 401–422. The McLaren Volume, Elsevier, Amsterdam.

Subramanian, M.A., Aravamudan, G., and Subba Rao, G.V. (1983) Oxide pyrochlores – A review. Progress in Solid State Chemistry, 15, 55–143.

Subramanian, M.A., Clearfield, A., Umarji, A. M., Shenoy, G.K., and Subba Rao, G.V. (1984) Synthesis and solid state studies on Mn_2Sb_2O7 and (Mn_{1-x} $Cd_x)_2Sb_2O_7$ pyrochlores. Journal of Solid State Chemistry, 52, 124–129.

Vitaliano, C. J. and Mason, B. (1952) Stibiconite and cervantite. American Mineralogist, 37, 982–999.

White, T.J. (1984) The microstructure and microchemistry of synthetic zirconolite, zirkelite and related phases. American Mineralogist, 69, 1156–1172.

Yakubovich, O.V., Urusov, V.S., Massa, W., Frenzen, G., and Babel, D. (1994). Crystal-chemical relations in weberite-group minerals, $Na_2M^{II}M^{III}F_7$, as derivatives of fluorite. Geologiya, 6, 19–25 (in Russian, English abstract).